

Nanoscale Porous Framework of Lithium Titanate for Ultrafast Lithium Insertion**

Johann M. Feckl, Ksenia Fominykh, Markus Döblinger, Dina Fattakhova-Rohlfing,* and Thomas Bein*

The rapidly growing demand for electric vehicles and mobile electronics urgently requires the development of electrochemical energy storage systems with both high energy density and high power.^[1] Supercapacitors^[2] can deliver very high powers, but their attainable energy densities are far lower than those of batteries.^[3] Closing the gap between the two main technologies requires the development of materials that can incorporate or liberate a large amount of charge in a very short time. Herein we report the synthesis of fully crystalline interconnected porous frameworks composed of ultrasmall lithium titanate spinel nanocrystals of a few nanometers in size. These frameworks feature a gravimetric capacity of about 175 mAh g⁻¹ at rates of 1–50 C (0.17–8.7 A g⁻¹) and can deliver up to 73% of their maximum capacity at unprecedented high rates of up to 800 C or 140 A g⁻¹ (corresponding to only 4.5 s of charge/discharge) without deterioration up to a thousand cycles. This titanate morphology results in the fastest ever-reported lithium insertion.

A key to this performance is the design of a fully crystalline interconnected porous framework composed of ultrasmall spinel nanocrystals of a few nanometers in size. The assembly of nanoscale building blocks into interconnected porous frameworks is a promising strategy to maximize the rate performance and to enhance the power density, and is also possible for materials not accessible by electrodeposition. Nanoscaling greatly increases the interface leading to enhanced charge transfer, and drastically shortens the ion/electron diffusion pathways by decreasing the grain size of the bulk material.^[1b,4,5] Lithium titanate Li₄Ti₅O₁₂ (LTO) is widely used as an active material in commercial lithium ion batteries and hybrid electrochemical storage devices^[6] owing to its suitable potential, relatively high capacity, and robustness. Although the lithium insertion rate in bulk LTO is intrinsically low, which is due to its low conductivity, recent reports have demonstrated that it can be substantially increased by

decreasing the crystal size to the nanometer scale,^[6,7] and several approaches were developed to obtain nanoscaled material. The reported strategies include flash annealing^[6] or solid-state reactions of nanosized titania,^[7a] which however lead to relatively large crystals of over 30 nm. Lithium titanate with much smaller crystalline domains and enhanced insertion rates can be obtained by solvothermal^[7b] and sol–gel reactions.^[7c–f,8] However, the power density and especially the cycling stability still need to be improved. High rate capability in combination with excellent cycling stability was achieved for hybrid materials composed of a few nanometer-sized crystals anchored on a conducting carbon matrix, although at the expense of significantly decreased gravimetric and volumetric capacities owing to a high content of the conducting support.^[9,10] A non-supported nanosized and fully crystalline LTO with extremely high insertion/extraction rates and high cycling stability has not yet been reported.

To create ultrasmall building blocks for a porous spinel framework, we have developed a solvothermal reaction in *tert*-butanol in the absence of water for the LTO synthesis. We have recently shown that *tert*-butanol is an excellent reaction medium for the synthesis of ultrasmall undoped and Nb-doped anatase titania crystals.^[5c,11] In a reaction of appropriate molecular metal oxide precursors (see below) with *tert*-butanol, the spinel nuclei are formed already at a low reaction temperature of 170 °C. Although the materials obtained at this temperature appear to be amorphous based on X-ray scattering, the formation of nuclei with the spinel symmetry can be detected by Raman spectroscopy (Figure 1a). The formed nuclei are subsequently crystallized in a controlled way by a thermal treatment of the dried reaction mixture at 400–500 °C. Screening of different precursor combinations demonstrates that a similar reactivity of the precursors in the solvothermal reaction is required for the formation of a pure spinel phase (Supporting Information, Figure S1). The choice of LiOtBu and Ti(OBu)₄ as the metal sources and the presence of amphiphilic Pluronic polymer (P123) in the reaction mixture were found to be essential for the formation of the phase-pure porous spinel framework. Moreover, considering that the single-phase LTO is formed only when the polymer is added, we can propose that it also influences the crystallization process, which is possibly due to its coordination to metal precursors, thus modulating their reactivity.

Heating the reaction mixture in air at 400 °C leads to the formation of a highly porous single-phase Li₄Ti₅O₁₂ spinel framework (named nano-LTO-400) with a very small size of the crystalline domains (3–4 nm), as derived from the peak broadening in the XRD patterns (Figure 1b) and from

[*] J. M. Feckl, K. Fominykh, Dr. M. Döblinger, Dr. D. Fattakhova-Rohlfing, Prof. Dr. T. Bein
Department of Chemistry and Center for Nanoscience (CeNS)
University of Munich (LMU)
Butenandtstrasse 11 (E), 81377 Munich (Germany)
E-mail: dina.fattakhova@cup.lmu.de
bein@lmu.de
Homepage: <http://bein.cup.uni-muenchen.de>

[**] Financial support from the NIM cluster and LMUMentoring is gratefully acknowledged. We thank Bastian Rühle for graphics design.

Supporting information for this article is available on the WWW under <http://dx.doi.org/10.1002/anie.201201463>.

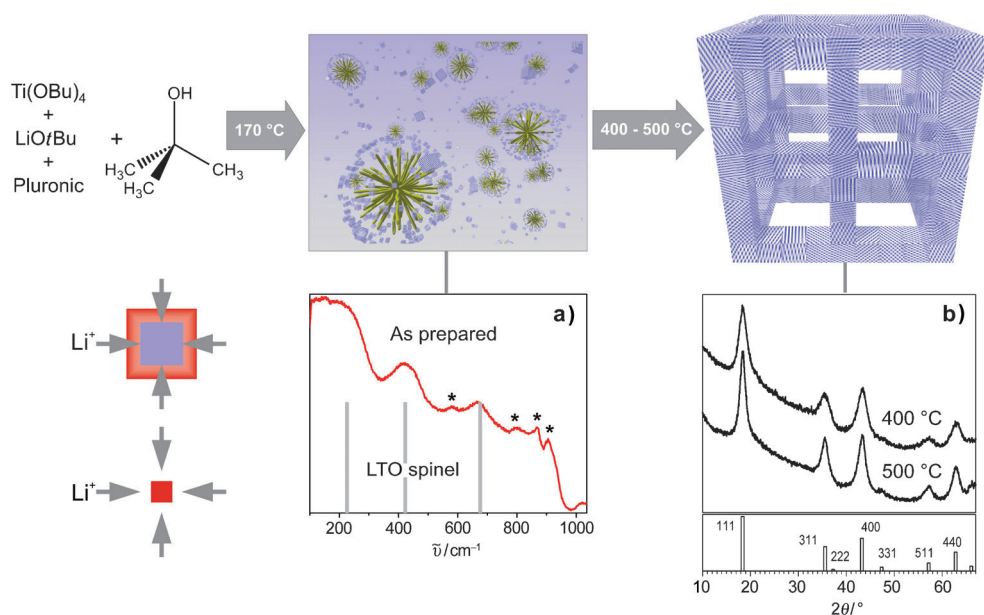


Figure 1. Formation of the lithium titanate LTO by solvothermal reaction in *tert*-butanol. a) Raman spectrum of the as-prepared material, demonstrating formation of the spinel nuclei after solvothermal reaction (gray bars: Raman bands of crystalline $\text{Li}_4\text{Ti}_5\text{O}_{12}$; remaining bands marked by an asterisk are associated with the Pluronic polymer). b) Powder XRD patterns of the LTO obtained after thermal treatment of as-prepared material at 400 °C and 500 °C and (below) the JCPDS card 26-1198 for the $\text{Li}_4\text{Ti}_5\text{O}_{12}$ spinel. Bottom left: the depth of Li diffusion (red) into large (top) and small (bottom) crystals.

transmission electron microscopy (Figure 2c). The heating time at this temperature does not markedly influence the crystallinity, as we did not observe any significant differences in the crystallinity of the material heated at 4 h and 12 h, respectively. Heating at 500 °C for 10 min (achieved with a 2 h ramp) leads to material, named nano-LTO-500, with slightly larger crystalline domains between 4 nm and 7 nm in diameter, but the highly porous character of the LTO framework remains preserved (Figure 1 b and 2 b,d). Electron microscopy confirms that the materials obtained at both temperatures are homogenous and that, despite the very small size of the crystals, the samples appear to be fully crystalline, being composed of spinel nanocrystals interconnected into a porous scaffold (Figure 2, SEM and TEM). Furthermore, gas adsorption studies show that the LTO samples obtained at 400 °C and at 500 °C feature highly porous morphologies with high surface areas of 205 m² g^{−1} and 170 m² g^{−1} and a uniform pore size of 7 nm and 8 nm (Figure 2), respectively. The latter correspond to the pores usually formed by Pluronic P123. Heating the as-prepared reaction mixture at 600 °C results in the formation of larger spinel crystals (around 35–55 nm) along with smaller crystals of (15 ± 5) nm in size, and in the formation of some fraction of larger TiO₂ anatase crystals (even for annealing times as short as 10 min; Supporting Information, Figure S2). The crystal growth at 600 °C is accompanied by the collapse of porosity and a decrease of surface area to 25 m² g^{−1}. These findings show that heating at 400–500 °C constitutes the optimum thermal treatment conditions for the nanoscale spinel materials using the above reaction procedure.

Coating of the synthesis solutions on conducting substrates followed by heating in air at temperatures beyond 400 °C leads to the formation of homogeneous films, the thickness of which can be varied from 150 to 500 nm (for experimental details, see the Supporting Information). The thickest films heated at 400 °C (nano-LTO-400) show a reversible electrochemical Li uptake of 176 mA h g^{−1}, which is practically equal to the theoretical insertion capacity for $\text{Li}_4\text{Ti}_5\text{O}_{12}$ spinel (Figure 3 a; the capacitive contribution from the FTO substrate can be practically neglected; Supporting Information, Figure S3). The maximum theoretical capacity was achieved already at a rate of 50 C or 8.6 A g^{−1} (meaning complete charging or discharging of the total storage capacity in 1/50 hour

or 1.2 min), and 96% of the maximum capacity were still achieved at the rate of 100 C or 17 A g^{−1} (36 s). At the rate of 300 C, up to 82% of the maximum capacity could still be obtained, and even at the very high rate of 400 C or 68 A g^{−1} (9 s) about 72% of the total capacity were still available (Figure 3 a). Even higher insertion/extraction rates can be achieved for the thinner films. The film of about 150 nm in thickness can be charged/discharged to 85% of its full capacity at the rate of 400 C and deliver up to 73% of the theoretical capacity at the rate of 800 C or 136 A g^{−1} (4.5 s) (Figure 4). We attribute this extremely high rate of insertion/extraction processes to the very small size of the crystalline domains and the very large electrode–electrolyte interface. The nanoscale morphology of the LTO spinel is also reflected in its potential profiles during charging (Li insertion) and discharging (Li extraction). Bulk $\text{Li}_4\text{Ti}_5\text{O}_{12}$ spinel exhibits an extended potential plateau owing to a well-defined two-phase insertion mechanism.^[12] In contrast, the nano-LTO-400 spinel shows curved voltage profiles with reduced length of the potential plateau region. This feature, which is characteristic for different nanosized materials, is usually attributed to a dominant role of surface-associated insertion processes in the very small crystals.^[12b,13] The latter involve a changed potential distribution in the near-surface area,^[12b] as well as pseudocapacitive surface storage processes, which become very significant for large-surface-area materials. Analysis of cyclic voltammograms of the nano-LTO-400 spinel performed according to the procedure described by Conway et al.^[14a] and Dunn et al.^[14b] reveals that the pseudocapacitive storage contributes to about 55–60% of the total charge, which can explain the unusually high rate performance of the nano-LTO

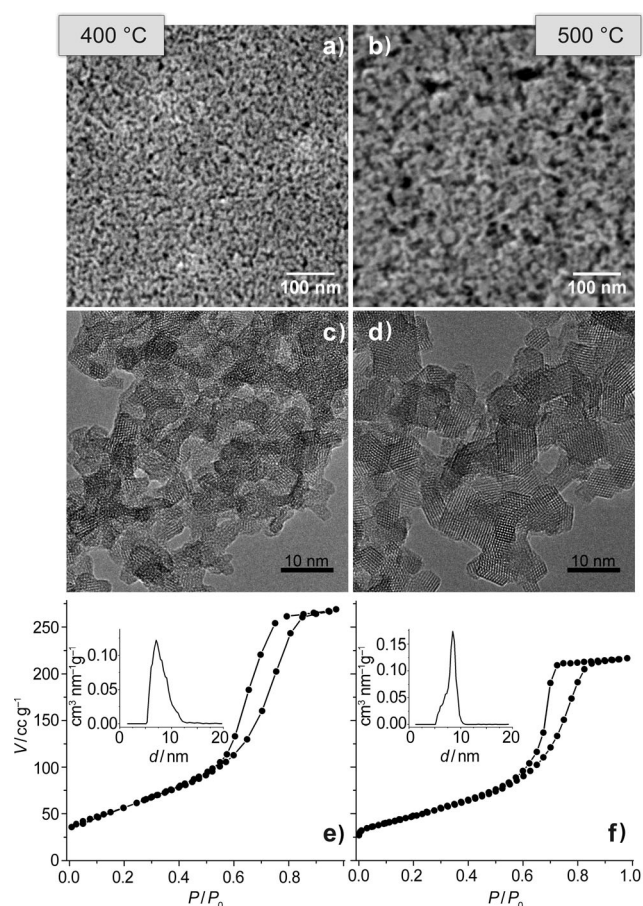


Figure 2. Morphology and crystallinity of nanosized spinel lithium titanate heated at 400 °C (a,c,e) and 500 °C (b,d,f): First row: SEM top view of the films on the FTO substrate; second row: HR-TEM images; third row: nitrogen sorption isotherms with pore size distributions.

electrodes (Supporting Information, Figure S4). Another feature of the nanocrystallinity is the additional insertion process at low potentials, which was also observed for other nanoscale spinel materials.^[12b] For the samples nano-LTO-400 and nano-LTO-500, this effect was observed for insertion rates below 25 C (4.3 A g^{-1}) at potentials below 1.2 V; this process is irreversible (Supporting Information, Figure S5). At high insertion rates, the insertion/extraction process in the nanosized spinel is perfectly reversible up to 1 V versus Li, and the electrode can be charged/discharged over several hundreds of cycles with only a minor capacity loss (the capacity retention is 98 % after 500 cycles and 89 % after 1000 cycles at a rate of 100 C; Figure 3c).

The lithium insertion behavior of the LTO annealed at 500 °C is similar to that of nano-LTO-400. Owing to the slightly increased crystal size (about 6 nm compared to about 3 nm for nano-LTO-400) the insertion/extraction rate in nano-LTO-500 is slightly slower compared to nano-LTO-400 but still extremely fast, such that 66 % of the maximum insertion capacity is retained at a rate of 400 C (68 A g^{-1}) and 80 % at a rate of 300 C (51 A g^{-1}), respectively, for about $0.5 \mu\text{m}$ thick films. The lower surface area of the nano-LTO-

500 material and the slightly larger crystal size are reflected in the increase of the plateau region (Figure 3b). The nano-LTO-500 spinel is also perfectly stable in multiple insertion/extraction processes (Figure 3c,d), the capacity retention being 98 and 91 % after 500 and 1000 cycles, respectively. We note that the high stability of these systems, even after 1000 cycles at 100 C (17 A g^{-1}), is reflected in unchanged nano-morphology (see electron micrographs in the Supporting Information, Figure S6). The advantages of the small crystal size for the lithium insertion rates are highlighted by comparing the electrochemical performance of the materials obtained after heating at 400 °C and 500 °C to that heated at 600 °C. In the latter, the presence of larger crystals in addition to the smaller crystals as well as the anatase impurity substantially decrease the insertion capacity already at low insertion rates to about 70 % of the theoretical value, and results in slower insertion kinetics (Supporting Information, Figure S2).

To the best of our knowledge, the nano-LTO spinel obtained by our novel *tert*-butanol route is by far the fastest spinel lithium titanate morphology for lithium insertion reported to date. It compares favorably with the porous nanocrystalline LTO spinel obtained by sol-gel methods,^[7c,8] composed of crystals greater than 11 nm (Figure 4). Our nano-LTO spinel also has a much higher insertion rate than porous $\text{Li}_4\text{Ti}_5\text{O}_{12}$ obtained by solution-combustion synthesis^[15] and carbon-coated nanocrystalline spinel,^[7g] and a higher available gravimetric capacity compared to hybrid materials.^[9,10] It is also significantly faster than the nanocrystalline TiO_2 (B) morphology that can deliver about 120 mA h g^{-1} at the rate of 20 A g^{-1} (60 C), which was recently reported to be the fastest titania material.^[16]

The novel non-aqueous synthesis in *tert*-butanol described herein enables the formation of extremely small crystalline nanoparticles of LTO whose size can be tuned by the heating temperature. We have shown that these particles can be used to construct crystalline lithium titanate spinel frameworks with extremely high surface areas already at the mild temperature of 400 °C. The combination of these features in the LTO framework leads to drastically enhanced kinetic behavior at high cycle stability. This way we have created materials with combined properties typical for both batteries (high energy density) and for supercapacitors (high power densities). The nano-LTO spinel can be charged very quickly to almost its full capacity, and then discharged at much slower rates (Supporting Information, Figure S7). Such materials are of great interest for applications in electrical vehicles or mobile electronic devices, where very short charging times are highly desirable and enabling for many envisioned applications. In combination with emerging fast nanostructured cathode materials,^[4,17] the ultrafast LTO anodes should have great potential for the development of lithium ion batteries and supercapacitors that can operate both at high energy density and high power.

Experimental Section

For the synthesis of nanocrystalline mesoporous LTO, stoichiometric amounts of titanium(IV) butoxide (2.04 g, 5.99 mmol), and lithium

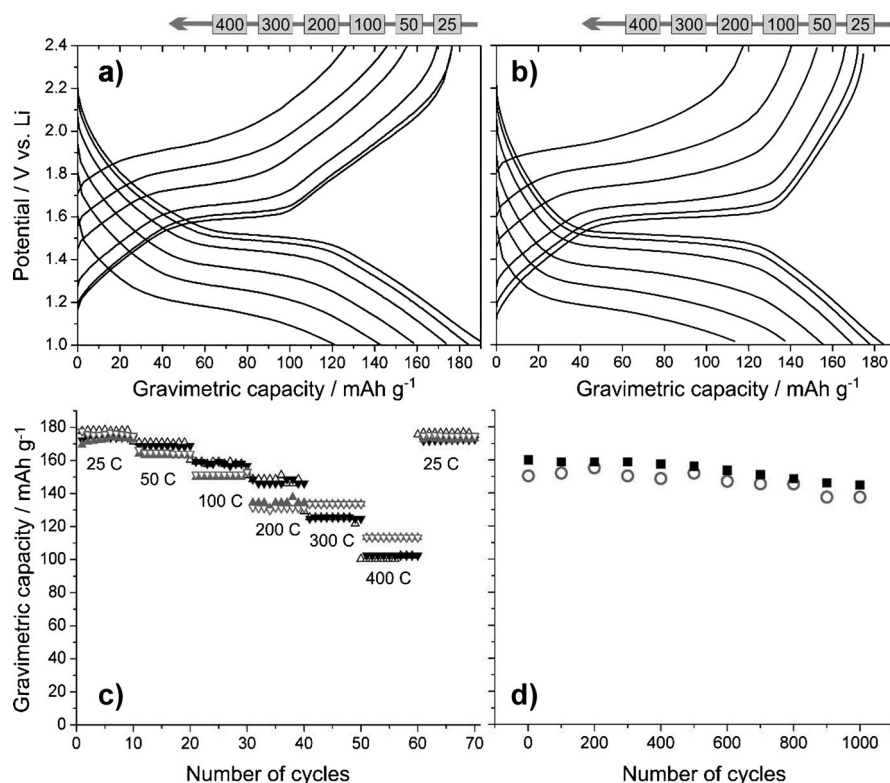


Figure 3. Electrochemical Li insertion/extraction with LTO spinel heated at 400°C (a) and at 500°C (b); galvanostatic charge/discharge is shown at different rates (corresponding to XC, with X shown in the corresponding label). c) Multicycling stability at different rates (ten cycles each are shown). d) Multicycling stability at a rate of 100 C (the capacity corresponds to the extraction process). The gray and black symbols correspond to the nano-LTO-400 and nano-LTO-500 spinel, respectively. The open and the filled symbols correspond to charge and discharge cycles, respectively. The cut-off potentials were 1.0 V and 2.4 V vs. Li. The thickness of the films is about 0.5 μm (corresponding to a loading of about 0.14 mg cm^{-2}).

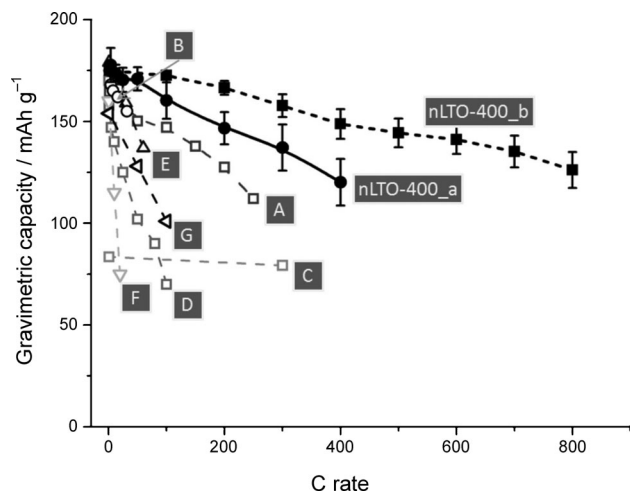


Figure 4. Rate capability of the nano-LTO-400 sample in comparison to previously reported fast LTO materials. mesoporous LTO (A, \square ;^[7d] and B, \circ),^[8] composite LTO–carbon–nanofiber material (C, \square ; the gravimetric capacity is calculated per total mass of the electrode material containing about 50% carbon),^[7h] LTO nanoparticles synthesized by the combustion method (D, \square),^[15] LTO prepared by a solvothermal method (E, Δ),^[7f] surface-modified LTO nanoparticles (F, ∇),^[7a] LTO/reduced graphite oxide nano-hybrid material (G, ∇).^[10] The materials cited above can have different thicknesses. Samples nLTO-400_a and nLTO-400_b denote the films with thickness of about 500 nm and 150 nm, respectively.

tert-butoxide (0.381 g, 4.76 mmol) were dissolved in *tert*-butanol (19 mL) containing Pluronic P123 (0.5 g) and benzyl alcohol (1 mL). The resulting solution was placed in a Teflon-lined steel autoclave and heated in a laboratory oven at 170°C for 20 h. Mesoporous films were prepared by drop-casting 5.0 μL of the as-prepared synthesis solution on about 1 cm^2 of FTO-coated glass substrates or, alternatively, by spin-coating at speeds of 500 to 2000 rpm at $(23 \pm 2)^\circ\text{C}$ and a relative humidity of $(35 \pm 10)\%$ (see the Supporting Information for more details). The transparent films were heated in air at various temperatures (nano-LTO-400: 2 h ramp to 400°C followed by 10 h dwell time; nano-LTO-500: 2 h ramp to 500°C followed by 10 min dwell time; nano-LTO-600: 1 h ramp to 600°C followed by 10 min dwell time). The thickness of the films can be varied from about 150 nm to about 500 nm by changing the rotation speed. The largest thickness of the films prepared by both methods is about 500 nm (corresponding to a loading of about 0.14 mg cm^{-2}).

Electrochemical measurements were carried out using a Parstat 2273 potentiostat (Princeton Applied Research). The measurements were performed in 1 M LiN(SO₂CF₃)₂ solution in a 1:1 by weight mixture of ethylenecarbonate (EC) and 1,2-dimethoxyethane (DME). Li wires were used as both the auxiliary and the reference electrodes.

Received: February 22, 2012

Revised: April 30, 2012

Published online: June 18, 2012

Keywords: lithium insertion · lithium titanate · nanocrystals · solvothermal synthesis · ultrafast materials

- a) Z. Yang, J. Zhang, M. C. W. Kintner-Meyer, X. Lu, D. Choi, J. P. Lemmon, J. Liu, *Chem. Rev.* **2011**, *111*, 3577–3613; b) V. Etacheri, R. Marom, R. Elazari, G. Salitra, D. Aurbach, *Energy Environ. Sci.* **2011**, *4*, 3243–3262; c) M. Contestabile, G. J. Offer, R. Slade, F. Jaeger, M. Thoenes, *Energy Environ. Sci.* **2011**, *4*, 3754–3772.
- J. R. Miller, P. Simon, *Science* **2008**, *321*, 651–652.
- R. J. Brodd, K. R. Bullock, R. A. Leising, R. L. Middaugh, J. R. Miller, E. Takeuchi, *J. Electrochem. Soc.* **2004**, *151*, K1K11.
- H. Zhang, X. Yu, P. V. Braun, *Nat. Nanotechnol.* **2011**, *6*, 277–281.
- a) A. S. Aricò, P. Bruce, B. Scrosati, J. M. Tarascon, W. Van Schalkwijk, *Nat. Mater.* **2005**, *4*, 366–377; b) F. Cheng, J. Liang, Z. Tao, J. Chen, *Adv. Mater.* **2011**, *23*, 1695–1715; c) J. M. Szeifert, J. M. Feckl, D. Fattakhova-Rohlfing, Y. Liu, V. Kalousek, J. Rathousky, T. Bein, *J. Am. Chem. Soc.* **2010**, *132*, 12605–12611.
- I. Plitz, A. DuPasquier, F. Badway, J. Gural, N. Pereira, A. Gmitter, G. G. Amatucci, *Appl. Phys. A* **2006**, *82*, 615–626.
- a) Y. Wang, H. Liu, K. Wang, H. Eiji, Y. Wang, H. Zhou, *J. Mater. Chem.* **2009**, *19*, 6789–6795; b) Y. Tang, L. Yang, Z. Qiu, J. Huang, *J. Mater. Chem.* **2009**, *19*, 5980–5984; c) L. Kavan, M. Gratzel, *Electrochem. Solid-State Lett.* **2002**, *5*, A39–A42; d) M.

- Kalbac, M. Zúkalová, L. Kavan, *J. Solid State Electrochem.* **2003**, *8*, 2–6; e) S.-H. Yu, A. Pucci, T. Hertrich, M.-G. Willinger, S.-H. Baek, Y.-E. Sung, N. Pinna, *J. Mater. Chem.* **2011**, *21*, 806–810; f) J. Lim, E. Choi, V. Mathew, D. Kim, D. Ahn, J. Gim, S.-H. Kang, J. Kim, *J. Electrochem. Soc.* **2011**, *158*, A275–A280; g) G.-N. Zhu, H.-J. Liu, J.-H. Zhuang, C.-X. Wang, Y.-G. Wang, Y.-Y. Xia, *Energy Environ. Sci.* **2011**, *4*, 4016–4022; h) K. Naoi, *Fuel Cells* **2010**, *10*, 825–833; i) E. Kang, Y. S. Jung, G.-H. Kim, J. Chun, U. Wiesner, A. C. Dillon, J. K. Kim, J. Lee, *Adv. Funct. Mater.* **2011**, *21*, 4349–4357.
- [8] J. Haetge, P. Hartmann, K. Brezesinski, J. Janek, T. Brezesinski, *Chem. Mater.* **2011**, *23*, 4384–4393.
- [9] K. Naoi, S. Ishimoto, Y. Isobe, S. Aoyagi, *J. Power Sources* **2010**, *195*, 6250–6254.
- [10] H.-K. Kim, S.-M. Bak, K.-B. Kim, *Electrochem. Commun.* **2010**, *12*, 1768–1771.
- [11] Y. Liu, J. M. Szeifert, J. M. Feckl, B. Mandlmeier, J. Rathousky, O. Hayden, D. Fattakhova-Rohlfing, T. Bein, *ACS Nano* **2010**, *4*, 5373–5381.
- [12] a) N. Takami, K. Hoshina, H. Inagaki, *J. Electrochem. Soc.* **2011**, *158*, A725–A730; b) W. J. H. Borghols, M. Wagemaker, U. Lafont, E. M. Kelder, F. M. Mulder, *J. Am. Chem. Soc.* **2009**, *131*, 17786–17792.
- [13] a) Y. G. Guo, Y. S. Hu, J. Maier, *Chem. Commun.* **2006**, 2783–2785; b) Y. S. Hu, L. Kienle, Y. G. Guo, J. Maier, *Adv. Mater.* **2006**, *18*, 1421–1426.
- [14] a) B. E. Conway, V. Birss, J. Wojtowicz, *J. Power Sources* **1997**, *66*, 1–14; b) J. Wang, J. Polleux, J. Lim, B. Dunn, *J. Phys. Chem. C* **2007**, *111*, 14925–14931.
- [15] A. S. Prakash, P. Manikandan, K. Ramesha, M. Sathiya, J. M. Tarascon, A. K. Shukla, *Chem. Mater.* **2010**, *22*, 2857–2863.
- [16] a) Y. Ren, Z. Liu, F. Pourpoint, A. R. Armstrong, C. P. Grey, P. G. Bruce, *Angew. Chem.* **2012**, *124*, 2206–2209; *Angew. Chem. Int. Ed.* **2012**, *51*, 2164–2167; b) H. Liu, Z. Bi, X.-G. Sun, R. R. Unocic, M. P. Paranthaman, S. Dai, G. M. Brown, *Adv. Mater.* **2011**, *23*, 3450–3454.
- [17] H.-W. Lee, P. Muralidharan, R. Ruffo, C. M. Mari, Y. Cui, D. K. Kim, *Nano Lett.* **2010**, *10*, 3852–3856.